Available online at www.sciencedirect.com
ScienceDirect
Journal of Chromatography B, 855 (2007) 98–103
JOURNAL OF CHROMATOGRAPHY B
www.elsevier.com/locate/chromb

MALDI-based imaging mass spectrometry revealed abnormal distribution of phospholipids in colon cancer liver metastasis☆

Shuichi Shimma[a,b], Yuki Sugiura[a,c,d], Takahiro Hayasaka[a], Yutaka Hoshikawa[e], Tetsuo Noda[e], Mitsutoshi Setou[a,b,c,d,*]

[a] *Okazaki Institute for Integrative Bioscience, National Institutes of Natural Sciences, Okazaki, Aichi 444-8787, Japan*
[b] *School of Life Science, The Graduate University for Advanced Studies, Okazaki, Aichi 444-8585, Japan*
[c] *Mitsubishi Kagaku Institute of Life Sciences (MITILS), Machida, Tokyo 194-8511, Japan*
[d] *Department of Bioscience and Biotechnology, Tokyo Institute of Technology, Yokohama, Kanagawa 226-8501, Japan*
[e] *The Genome Center of Japanese Foundation for Cancer Research, Koutou-ku, Tokyo 135-8550, Japan*

Received 29 September 2006; accepted 6 February 2007
Available online 28 February 2007

Abstract

We present the results of matrix-assisted laser desorption/ionization (MALDI) imaging and direct molecular identification using tandem mass spectrometry (MS/MS) in colon cancer liver metastasis. Cancer tissue was removed from a Japanese patient and frozen immediately without any fixations. The sections were sliced to a thickness of 3 μm. The matrix for lipid ionization was 2,6-dihydroxy acetophenone. The matrix solution was applied with an airbrush into a thin uniform matrix layer on the tissue surface. After two-dimensional laser scanning, the images were reconstructed as a function of *m/z* from a few hundred obtained spectra. In the obtained images, the existence of molecules was represented by a pseudo-color corresponding to the signal intensity. In a feasibility study, we picked up a localized signal, *m/z* 725 in a cancerous area. The MS/MS result suggested that *m/z* 725 was sphingomyelin(16:0)+Na. Thus, we successfully show the feasibility of MALDI imaging as a tool for the analysis of pathological specimens.

Keywords: Imaging mass spectrometry; Colon cancer; Phospholipids; Sphingomyelin; Aging; Molecular imaging

1. Introduction

Colon cancer is a frequent cause of mortality and morbidity in developed, developing, and industrialized countries. The incidence rate of colon cancer has been rising rapidly in Japan [1]. Aging increases the incidence of colorectal cancer [2], and genealogy is also a factor [3]. Diet is an important environmental factor, and a high intake of animal protein and fat along with a low intake of fiber increases the risk of colon cancer [4].

A number of approaches have been taken to treat colon cancer and to understand its biology and causes. An approach using a cDNA microarray has revealed some biological characteristics of cancer cells, such as specific gene expression for drug resistance [5]. A histochemical study with hematoxylin and eosin (HE) staining has shed light on the staging of colon cancer [6]. Pharmacological analyses have shown the effects of drug treatment and localization [7]. However, the causes of this cancer's origination and progression are not completely understood.

Researchers have also made great efforts to identify biomolecules differentially expressed in cancerous and normal tissues, which can be utilized as biomarkers [8,9]. In particular, we have considered phospholipids, which play important roles in the composition of the cell membrane, as important molecules to investigate in colon cancer [10]. It is generally accepted that the membrane characteristics are determined by components of phospholipid species and that the composition of these species is strictly determined by components of phospholipid species [10].

Previous studies reported that cancerous tissue contains elevated total amounts of all phospholipids [11] as well as altered phospholipid composition of the membrane [11,12]. In addi-

☆ This paper was presented at the 31st Annual Meeting of the Japanese Society for Biomedical Mass Spectrometry, Nagoya, Japan, 28–29 September 2006

* Corresponding author.
E-mail address: setou@nips.ac.jp (M. Setou).

1570-0232/$ – see front matter © 2007 Elsevier B.V. All rights reserved.
doi:10.1016/j.jchromb.2007.02.037

tion, differences in the composition between cancer cells with metastases and non-metastatic were determined using high-performance liquid chromatography (HPLC) [12]. Furthermore, the elevated activity of enzymes (phospholipase A) altered fatty acid composition of phospholipids [13]. These reports indicate that phospholipids can be utilized as a useful marker for the detection of colon cancer.

Direct mass spectrometry (MS) of biological tissues using matrix-assisted laser desorption/ionization (MALDI) can profile biological molecules including subtypes of phospholipids [14]. In addition, highly accurate MS can profile fatty acids, which comprise phospholipids. Moreover, this approach can be expanded to imaging mass spectrometry (MALDI imaging), which can visualize the distribution of individual biomolecules in a tissue section [15–17]. The technique has been applied to pathological specimens including Alzheimer's [18,19] and Parkinson's [20,21] disease, muscular dystrophy [22], and lung cancer [23].

In this study, we aimed to show the feasibility of MALDI imaging as a tool for the pathological specimens. We applied the technique to human colon cancer liver metastasis. Two phospholipids were visualized as differentially expressed molecules between the cancerous and normal areas. We also show the result of tandem mass spectrometry (MS/MS) to identify the molecule localized in the cancerous area.

2. Experimental

2.1. Chemicals

Trifluoroacetic acid (TFA) was purchased from Merck (Darmstadt, Germany). Methanol was purchased from Wako Pure Chemical Industries (Osaka, Japan). 2,6-Dihydroxy acetophenone (2,6-DHA) was purchased from Bruker Daltonics (Leipzig, Germany). A calibration standard for the low *m/z* region was prepared by mixing angiotensin III ($[M+H]^+$: 899.47) and Leu-Euk ($[M+H]^+$: 556.28). Distilled water, purified by a Milli-Q water system (Millipore, Bedford, MA, USA), was used for the preparation of all buffers and solvents. All the chemicals used in this study were of the highest purity available.

2.2. Conductive sheet

The conductive sheet was purchased from Tobi Co., Ltd. (Osaka, Japan). This sheet has a thin indium-tin-oxide (ITO) layer on a polyethylene terephthalate. The sheet was 125 μm thick and its conductivity was 100 Ω. The transparency was 80% ($\lambda = 550$ nm), so that we could observe stained tissues with transmitted light. This flexible sheet made sample handling easy, because the sheet could be cut to an arbitrary size with a paper cutter and samples did not crack easily, which was sometimes problematic with glass slides.

2.3. Tissue block preparation

A tissue block with colon cancer liver metastasis was removed from a Japanese patient during an operation, and rinsed with PBS buffer. The tissue was frozen in liquid nitrogen immediately to minimize degradation and was kept at −80 °C. Informed consent was obtained before the operation.

2.4. Workflow of imaging mass spectrometry

The workflow of MALDI imaging and identification is shown in Fig. 1. Frozen thin sections were sliced and mounted on conductive materials. One tissue section was stained (Fig. 1(a)), and another section was used for MALDI imaging (Fig. 1(b)). The obtained spectra were accumulated and compared between normal and abnormal areas (Fig. 1(c)). The distribution map was reconstructed from an ion of interest (Fig. 1(d)). Using obtained images, MS/MS was performed on the localized area, and we assigned lipid species (Fig. 1(e)).

2.5. Sample preparation

Before sectioning, the liver block was left for 30 min at −20 °C. The tissue sections were sliced to a thickness of 3 μm using a cryostat (CM 3050; Leica, Wetzler, Germany) and mounted onto the ITO sheet. A thin matrix layer was applied to the surface by an airbrush. A two-minute spraying of 2,6-DHA solution (30 mg/ml in 70%methanol/0.1%TFA) was iterated

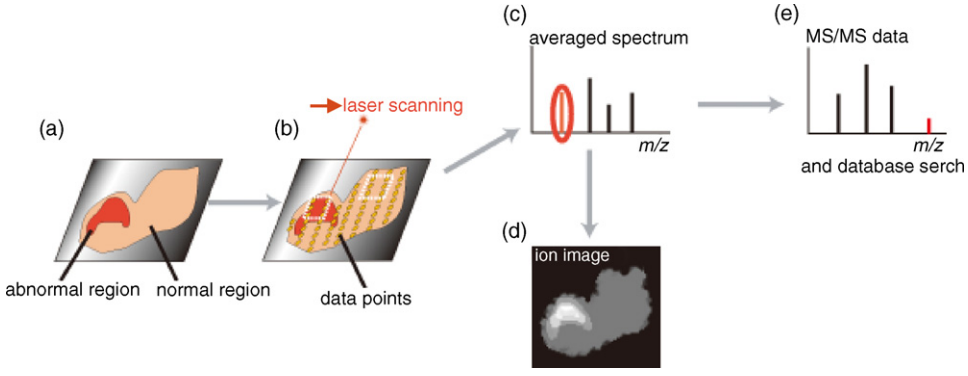

Fig. 1. Workflow of imaging mass spectrometry. Two sections were sliced (typical thickness <5 μm) using a cryostat and were placed on the conductive material. One section was for histochemical staining (a), and the other was for MALDI imaging. (b). Obtained spectra were accumulated and compared between the normal and abnormal areas (c). The ion image for the specific signals was reconstructed from the obtained spectra (d). MS/MS analysis and a database search were performed for molecular identification (e).

twice. During spraying, the distance between the nozzle and the tissue surface was kept at 15 cm. After drying, the ITO sheet was attached to a metal-coated glass slide by conductive tape to facilitate electrical conduction.

2.6. Conditions of mass spectrometry and MALDI imaging

The tissue section was analyzed using a MALDI-time-of-flight/time-of-flight (MALDI-TOF/TOF)-type instrument, Ultraflex II TOF/TOF (Bruker Daltonics, Leipzig, Germany), which was equipped with a Nd:YAG laser with a 200 Hz repetition rate. To install the metal-coated glass slides in the ionization chamber, we used a special holder (MTP Slide-Adapter 2, Bruker Daltonics), which had concavities to hold the slides.

External calibration solution was deposited on the surface of the ITO sheet to minimize mass shift. The laser irradiated the calibration spot with 500 shots in the positive ion reflector mode. In this experiment, the parameters of the mass spectrometer were set to obtain the highest sensitivity for *m/z* 0–2000. In this experiment, an acceleration voltage set to 25 kV and laser power was 39% (Bruker's notation).

A raster scan on the tissue surface was performed automatically. Laser irradiation consisted of 100 shots in each spot. The interval of data points was 100 μm, giving a total of 445 data points in the tissue section. The spectra shown in Section 3 were accumulated in square sections (300 μm × 300 μm) of normal and cancerous areas. Here, we did not apply data processing such as smoothing or baseline subtraction. The reconstructions from the spectra were performed by FlexImaging (Bruker Daltonics).

2.7. Lipid identification

To identify lipid species, we performed MS/MS and analyze the peak pattern. In the positive ion mode, the lipids which had phosphocholine were mainly detected as a result of positive charge in nitrogen of trimethylamine. We confirmed the pattern of phosphocholine in MS/MS data, after that we used a database, Lipid Search (http://lipidsearch.jp/manual_search/), to determine the compositions of fatty acid.

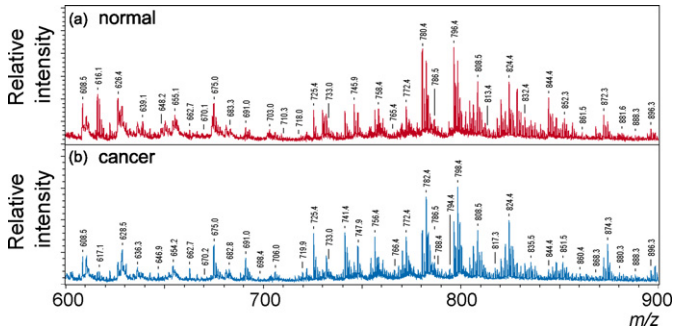

Fig. 3. Comparison of accumulated spectra from the normal (a) and cancerous (b) areas. The spectra were compared in the range of *m/z* 600–900, corresponding to the *m/z* of phospholipids.

3. Results and discussion

3.1. Comparison of HE staining tissue with MALDI imaging tissue

One tissue section with colon cancer liver metastasis was stained with HE to distinguish between normal and cancerous areas (Fig. 2(a)). The staining showed that normal, stroma, and cancer cells were localized on the left, middle, and right of the tissue section, respectively. Another tissue section was mounted on an ITO sheet, to which a DHA solution was applied as a matrix for lipid ionization. According to the stained tissue, two quadrate areas – one from the normal area and the other from the cancerous area – were selected to accumulate the obtained spectra (Fig. 2(b)).

3.2. Comparison of accumulated spectra in normal and cancerous areas

Fig. 3 shows the accumulated spectra from the normal area (Fig. 3a) and the cancerous area (Fig. 3b). Both spectra had

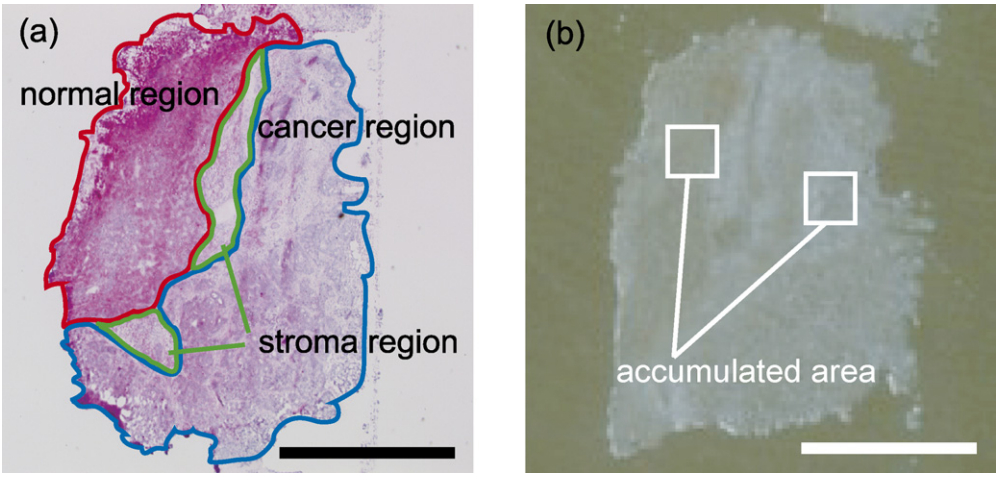

Fig. 2. Comparison of HE-stained tissue section and tissue section prepared for MALDI imaging. The HE-stained section showed that normal, stroma, and cancer cells were localized on the left, middle, and right on the section, respectively (a). The tissue section prepared for MALDI imaging (b). From the data points in white squares in (b), mass spectra were accumulated and are presented in Fig. 3. Bars, 1 mm.

a large number of signals in the mass range, corresponding to the phospholipids region [24]. Major signals were assigned to the phospholipids, especially to phosphatidylcholine (PC) and sphingomyelin (SM) [24].

A lot of signals were different between the normal and cancerous areas. We made a summary table of peaks (Table 1). The *t*-test was performed on a data set between normal and cancerous region. In the following discussion we focused on the signal at *m/z* 725 which had lower expression in the normal area than in the cancerous area.

3.3. Ion distribution images

The ion images of *m/z* 725 were reconstructed to reveal the distribution on the cancerous tissue section (Fig. 4(a)). The ion image of *m/z* 616 shown in Fig. 4(b) was localized in the normal region. The imaging result of *m/z* 616 supported that the localization of *m/z* 725 did not come from the concentration of sprayed matrix. The merger of the ion images of *m/z* 616 and *m/z* 725 revealed that both biomolecules were colocalized in the stroma area (Fig. 4(c)).

In this imaging experiment, it took about 60 min to complete laser scanning. The number of data points was 445 in tissue section (2.0 mm × 2.5 mm). The data acquisition (DAQ) time depended on the number of data points and laser shots. The number of data points and laser shots were variable parameters for operators. To visualize rough distributions of molecules, the DAQ time could be shortened (to approximately less than 10 min) by changing the parameters. This presents an advantage over histochemical staining, which require several steps and a lot of time. Another feature of MALDI imaging is that it can obtain many images at a time from one specimen. As shown in Fig. 3, a large number of signals were recorded. Therefore, we could make images from all signals in a few minutes. Obtaining all images with the same operation condition could minimize artifacts and ensure reproducibility among obtained images. We believe that MALDI imaging is a good tool for analyzing pathological specimens.

3.4. Lipid assignment with MS/MS data

The result of MS/MS with regard to *m/z* 725 in the cancerous area showed peaks of *m/z* 666.5 and 542.5. The peak of *m/z* 666.5 corresponded to neutral loss of trimethylamine (59 u, C_3H_9N), and the peak of *m/z* 542.5 corresponded to neutral loss of trimethylamine and cyclophosphate (124 u, $C_2H_5O_4P$). This result indicated that *m/z* 725 contained an alkali metal adduct phosphocholine, therefore, *m/z* 725 was PC or SM species [25]. Applying the nitrogen rule to phospholipids, the odd nominal mass indicated SM because of the presence of an additional nitrogen in the sphingosine of SM. We concluded that *m/z* 725 was determined to be an SM species. The Lipid Search suggested that *m/z* 725 corresponded to SM(16:0) + Na (Fig. 5).

In a recent study, proteins in colon cancer were identified using a conventional proteomics procedure [26]. However, phos-

Table 1
Summary table of different peak between normal and cancerous region

m/z	Intensity (counts)		*P*-value	
	Normal	Cancer		
608.5	4226.3 ± 760.6	2266.5 ± 351.4	0.016	*
616.1	3619.2 ± 526.0	1251.1 ± 241.8	0.003	**
617.1	3785.6 ± 595.7	1247.5 ± 258.8	0.003	**
626.4	5421.3 ± 912.3	2913.6 ± 412.5	0.014	*
628.5	3967.3 ± 680.6	5347.6 ± 735.4	0.010	*
636.3	2020.7 ± 326.5	2311.6 ± 386.9	0.471	
639.1	1332.4 ± 202.2	1330.4 ± 200.8	0.993	
646.9	500.4 ± 118.8	523.8 ± 119.8	0.733	
648.2	1332.0 ± 248.2	463.6 ± 71.8	0.003	**
654.2	2503.5 ± 414.0	2572.6 ± 351.3	0.851	
655.1	2253.9 ± 374.3	2066.0 ± 272.9	0.646	
662.7	382.2 ± 79.2	486.4 ± 95.7	0.164	
670.1	271.8 ± 37.0	428.0 ± 78.8	0.027	*
675.0	2856.4 ± 572.1	4785.3 ± 752.2	0.041	*
682.8	814.0 ± 146.8	1525.0 ± 203.6	0.024	*
683.3	1041.0 ± 159.7	1360.3 ± 188.0	0.110	
691.0	750.2 ± 133.5	3287.5 ± 634.2	0.003	**
698.4	218.4 ± 24.4	381.8 ± 85.7	0.063	
703.0	759.8 ± 106.4	681.3 ± 182.0	0.646	
706.0	601.3 ± 118.4	1559.9 ± 259.6	0.004	**
710.3	210.9 ± 30.2	416.6 ± 80.2	0.025	*
718.0	221.6 ± 25.1	811.8 ± 163.4	0.005	**
719.9	347.2 ± 46.4	1221.7 ± 224.8	0.005	**
725.4	1101.9 ± 169.4	4150.7 ± 741.0	0.002	**
733.0	835.9 ± 138.5	1588.9 ± 261.5	0.011	*
741.4	938.0 ± 168.4	4368.7 ± 852.0	0.003	**
745.9	2115.6 ± 387.8	1912.1 ± 331.7	0.662	
747.9	1607.3 ± 278.8	3818.6 ± 659.3	0.008	**
756.4	1151.1 ± 174.7	3236.6 ± 470.2	0.002	**
758.4	1540.1 ± 231.3	2292.2 ± 313.3	0.056	
765.4	357.1 ± 54.7	499.8 ± 119.0	0.241	
766.4	348.8 ± 58.3	842.1 ± 145.9	0.015	*
772.4	1112.4 ± 174.9	3440.8 ± 605.9	0.005	**
780.4	3521.7 ± 678.4	2663.2 ± 384.5	0.265	
782.4	3235.9 ± 560.9	5607.4 ± 807.3	0.028	*
786.5	1146.7 ± 175.1	2037.8 ± 301.2	0.017	*
788.4	665.3 ± 75.3	1328.2 ± 187.1	0.005	**
794.4	775.5 ± 158.1	907.9 ± 155.1	0.574	
796.4	3341.6 ± 627.3	3287.4 ± 493.8	0.944	
798.4	2833.4 ± 464.8	5939.2 ± 854.9	0.009	**
808.5	2445.3 ± 430.0	3212.2 ± 434.9	0.194	
813.4	377.8 ± 66.3	756.8 ± 100.4	0.002	**
817.3	251.2 ± 36.2	601.0 ± 107.6	0.003	**
824.4	2457.5 ± 463.1	3524 ± 507.2	0.125	
832.4	971.1 ± 168.0	1157.8 ± 201.5	0.446	
835.5	779.2 ± 129.1	1380.2 ± 204.3	0.010	*
844.4	1455.6 ± 292.4	853.3 ± 183.8	0.106	
851.5	671.1 ± 108.0	1505.1 ± 263.5	0.012	*
852.3	917.1 ± 184.9	1159.0 ± 180.6	0.334	
860.4	232.0 ± 26.4	501.2 ± 67.8	0.005	**
861.5	277.3 ± 42.5	515.8 ± 72.8	0.012	*
868.3	397.0 ± 77.3	384.1 ± 68.0	0.841	
872.3	884.6 ± 159.2	789.0 ± 192.4	0.527	
874.3	483.0 ± 125.6	991.4 ± 230.6	0.011	*
880.3	483.0 ± 125.6	430.5 ± 63.8	0.084	
881.6	286.3 ± 56.8	419.3 ± 81.7	0.126	
888.3	203.2 ± 24.7	493.6 ± 65.6	0.002	**
896.3	374.7 ± 79.1	501.7 ± 96.7	0.095	

The "*" indicated "$P < 0.05$" and "**" indicated "$P < 0.01$".

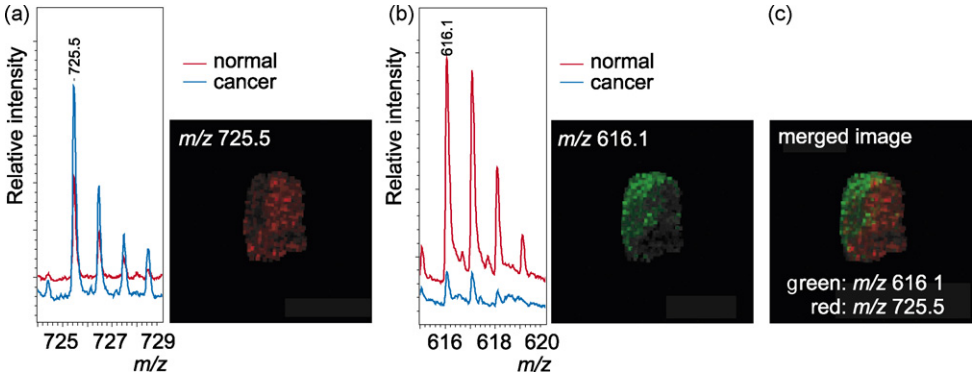

Fig. 4. The results of ion image. The signal at *m/z* 725 showed higher expression in the cancerous area than in the normal area (a). Ion image revealed the strong distribution of ion at *m/z* 616 in the normal area (b). Images of localized molecules in cancerous and normal area indicated that these results were not derived from the ununiformity of matrix concentration. The merged image was reconstructed from the images at *m/z* 616 and 725 (c). It shows that both biomolecules were present in the stroma area. Red and green dots indicate the presence of biomolecules corresponding to *m/z* 725 and *m/z* 616.

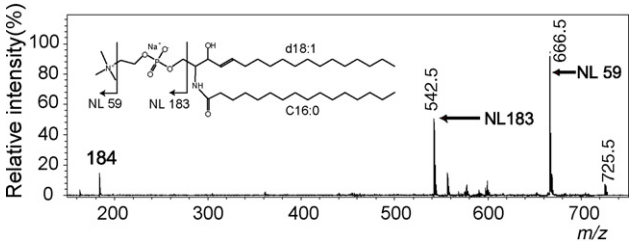

Fig. 5. MS/MS data of *m/z* 725. The neutral loss of 59 u and 124 u observed in the spectra is trimethylamine and cyclophosphate, indicating phosphocholine structure. This fragmentation occurred when alkali metal was adducted the precursor ion. The biomolecule of *m/z* 725 was assumed to be SM(16:0) + Na.

pholipids have not been reported, especially using direct tissue MS. We showed that SM(16:0) was strongly expressed in the cancerous area. Brasitus et al. reported the relationship between colorectal cancer and lipids [27]. According to their report, they used colonocyte of rats treated with 1,2-dimethylhydrazine (DMH). Their results suggested that the lipid compositions were altered as duration of treatment with DMH which progress the malignancy was longer. Moreover, only sphingomyelin was increased significantly. Our result was consistent with such a biochemical approach.

4. Conclusion

We presented a MALDI imaging procedure and its results for the analysis of human colon cancer liver metastasis. MS/MS analysis of molecules in the normal and cancerous areas suggested that SM(16:0) was accumulated in cancer cells. We have successfully shown the feasibility of MALDI imaging as a tool for the analysis of pathological specimens. The lipid imaging without any biological probes will bring novel findings which are not obtained by conventional techniques.

Acknowledgements

The authors would like to thank M. Sugiyama in the Genome Center of JFCR for her technical support with histochemical staining. This work was supported by a Grant-in-Aid for SENTAN (M.S.) from Japan Science and Technology Agency.

References

[1] W. Ajiki, H. Tsukuma, A. Oshima, Jpn. J. Clin. Oncol. 34 (2004) 352.
[2] G.R. Newell, M.R. Spitz, J.G. Sider, Semin. Oncol. 16 (1989) 3.
[3] L. Harkins, A.L. Volk, M. Samanta, I. Mikolaenko, W.J. Britt, K.I. Bland, C.S. Cobbs, Lancet 360 (2002) 1557.
[4] K. Wakai, K. Hirose, K. Matsuo, H. Ito, K. Kuriki, T. Suzuki, T. Kato, T. Hirai, Y. Kanemitsu, K. Tajima, J. Epidemiol. 16 (2006) 125.
[5] S. Huerta, D.M. Harris, A. Jazirehi, B. Bonavida, D. Elashoff, E.H. Livingston, D. Heber, Int. J. Oncol. 22 (2003) 663.
[6] L. Di Marzio, A. Di Leo, B. Cinque, D. Fanini, A. Agnifili, P. Berloco, M. Linsalata, D. Lorusso, M. Barone, C. De Simone, M.G. Cifone, Cancer Epidemiol. Biomarkers Prev. 14 (2005) 856.
[7] R. Saito, J.R. Bringas, T.R. McKnight, M.F. Wendland, C. Mamot, D.C. Drummond, D.B. Kirpotin, J.W. Park, M.S. Berger, K.S. Bankiewicz, Cancer Res. 64 (2004) 2572.
[8] R. Alessandro, C. Belluco, E.C. Kohn, Clin. Colorectal Cancer 4 (2005) 396.
[9] J.L. Westra, J.T. Plukker, C.H. Buys, R.M. Hofstra, Clin. Colorectal Cancer 4 (2004) 252.
[10] P.R. Cullis, D.B. Fenske, M.J. Hope, Biochemistry of Lipids, Lipoproteins and Membranes, Elsevier, 1991.
[11] D.A. Dueck, M. Chan, K. Tran, J.T. Wong, F.T. Jay, C. Littman, R. Stimpson, P.C. Choy, Mol. Cell. Biochem. 162 (1996) 97.
[12] I. Dobrzynska, B. Szachowicz-Petelska, S. Sulkowski, Z. Figaszewski, Mol. Cell. Biochem. 276 (2005) 113.
[13] M. Okita, D.C. Gaudette, G.B. Mills, B.J. Holub, Int. J. Cancer 71 (1997) 31.
[14] A.S. Woods, S.N. Jackson, Aaps J. 8 (2006) E391.
[15] M. Stoeckli, P. Chaurand, D.E. Hallahan, R.M. Caprioli, Nat. Med. 7 (2001) 493.
[16] M. Stoeckli, T.B. Farmer, R.M. Caprioli, J. Am. Soc. Mass Spectrom. 10 (1999) 67.
[17] R.M. Caprioli, T.B. Farmer, J. Gile, Anal. Chem. 69 (1997) 4751.
[18] T.C. Rohner, D. Staab, M. Stoeckli, Mech. Ageing Dev. 126 (2005) 177.
[19] M. Stoeckli, D. Staab, M. Staufenbiel, K.H. Wiederhold, L. Signor, Anal. Biochem. 311 (2002) 33.
[20] J. Pierson, P. Svenningsson, R.M. Caprioli, P.E. Andren, J. Proteome Res. 4 (2005) 223.
[21] J. Pierson, J.L. Norris, H.R. Aerni, P. Svenningsson, R.M. Caprioli, P.E. Andren, J. Proteome Res. 3 (2004) 289.
[22] D. Touboul, A. Brunelle, F. Halgand, S. De La Porte, O. Laprevote, J. Lipid Res. 46 (2005) 1388.

[23] K. Yanagisawa, Y. Shyr, B.J. Xu, P.P. Massion, P.H. Larsen, B.C. White, J.R. Roberts, M. Edgerton, A. Gonzalez, S. Nadaf, J.H. Moore, R.M. Caprioli, D.P. Carbone, Lancet 362 (2003) 433.
[24] T.J. Garrett, R.A. Yost, Anal. Chem. 78 (2006) 2465.
[25] F.F. Hsu, J. Turk, J. Am. Soc. Mass Spectrom. 14 (2003) 352.
[26] P. Chaurand, B.B. DaGue, R.S. Pearsall, D.W. Threadgill, R.M. Caprioli, Proteomics 1 (2001) 1320.
[27] T.A. Brasitus, P.K. Dudeja, R. Dahiya, J. Clin. Invest. 77 (1986) 831.